



HAL
open science

Network analyses reveal negative link between changes in adipose tissue GDF15 and BMI during dietary-induced weight loss

Alyssa Imbert, Nathalie Vialaneix, Julien Marquis, Julie Vion, Aline Charpagne, Sylviane Metairon, Claire Laurens, Cedric Moro, Nathalie Boulet, Ondine Walter, et al.

► To cite this version:

Alyssa Imbert, Nathalie Vialaneix, Julien Marquis, Julie Vion, Aline Charpagne, et al.. Network analyses reveal negative link between changes in adipose tissue GDF15 and BMI during dietary-induced weight loss. *Journal of Clinical Endocrinology and Metabolism*, 2022, 107 (1), pp.e130-e142. 10.1210/clinem/dgab621 . hal-03540946

HAL Id: hal-03540946

<https://hal.inrae.fr/hal-03540946>

Submitted on 24 Jan 2022

HAL is a multi-disciplinary open access archive for the deposit and dissemination of scientific research documents, whether they are published or not. The documents may come from teaching and research institutions in France or abroad, or from public or private research centers.

L'archive ouverte pluridisciplinaire **HAL**, est destinée au dépôt et à la diffusion de documents scientifiques de niveau recherche, publiés ou non, émanant des établissements d'enseignement et de recherche français ou étrangers, des laboratoires publics ou privés.

Title:

Network analyses reveal negative link between changes in adipose tissue GDF15 and BMI during dietary induced weight loss

Authors:

Alyssa Imbert^{1,2,3*}, Nathalie Vialaneix^{3*}, Julien Marquis⁴, Julie Vion^{1,2}, Aline Charpagne⁵, Sylviane Metairon⁵, Claire Laurens^{1,2}, Cedric Moro^{1,2}, Nathalie Boulet^{1,6}, Ondine Walter⁵, Grégory Lefebvre⁵, Jörg Hager⁵, Dominique Langin^{1,2,7,8}, Wim HM Saris⁹, Arne Astrup¹⁰, Nathalie Viguerie^{1,2,7§}, Armand Valsesia^{5§}

* equal contribution, § joint supervision

Affiliations:

¹ Institut National de la Santé et de la Recherche Médicale (Inserm), UMR1297, Institute of Metabolic and Cardiovascular Diseases, Team Metabolic Disorders and Diabetes, 31400, Toulouse, France;

² University of Toulouse, UMR1297, Institute of Metabolic and Cardiovascular Diseases, Paul Sabatier University, 31400, Toulouse, France;

³ INRAE, UR875 Mathématiques et Informatique Appliquées Toulouse, F-31326 Castanet-Tolosan, France ;

⁴ Université de Lausanne, Genomic Technologies Facility, 1015, Lausanne, Switzerland

⁵ Nestlé Institute of Health Sciences, Metabolic Health Department, 1015, Lausanne, Switzerland

⁶ Institut National de la Santé et de la Recherche Médicale (Inserm), UMR1297, Institute of Metabolic and Cardiovascular Diseases, Team Adipose tissue, microbiota and cardiometabolic flexibility, 31400, Toulouse, France;

⁷ Franco-Czech Laboratory for Clinical Research on Obesity, Third Faculty of Medicine, Prague and Paul Sabatier University, Toulouse, France;

⁸ Toulouse University Hospitals, Laboratory of Clinical Biochemistry, 31000, Toulouse, France;

⁹ Department of Human Biology, NUTRIM School of Nutrition and Translational Research in Metabolism, Maastricht University Medical Centre, Maastricht, The Netherlands;

¹⁰ Department of Nutrition, Exercise and Sports, Faculty of Sciences, University of Copenhagen, Denmark.

Short Title:

Human adipose tissue GDF15 upregulation with diet

Keywords:

Adipocyte, macrophage, weight loss, network analyses, low calorie diet, inflammation

Correspondence : armand.valsesia@gmail.com; nathalie.viguerie@inserm.fr

Grants:

This work was supported by Inserm, Paul Sabatier University, the Innovative Medicines Initiative Joint Undertaking (grant agreement n° 115372), and the Commission of the European Communities (FP6-513946 DiOGenes).

Disclosure Summary: DL is a member of Institut Universitaire de France; JM, AC, SM, OW, GL, JH and AV are full-time employee at Nestlé; WHMS reports having received research support from several food companies such as Nestlé, DSM, Unilever, Nutrition et Santé and Danone as well as Pharmaceutical companies such as GSK, Novartis and Novo Nordisk; he is an unpaid scientific advisor for the International Life Science Institute, ILSI Europe. AA reports grants and personal fees from Global Dairy Platform, personal fees from McCain Foods, McDonald's, Arena Pharmaceuticals Inc., Basic Research, Dutch Beer Knowledge Institute, Netherlands, Gelesis, Novo Nordisk, Denmark, Orexigen Therapeutics Inc., S-Biotek, Denmark, Twinlab and Vivus Inc., grants from Arla Foods, Denmark, Danish Dairy Research Council and Nordea Foundation, Denmark, outside the submitted work, and royalties received for the book first published in Danish as 'Verdens Bedste Kur' (Politiken; Copenhagen, Denmark), and subsequently published in Dutch as 'Het beste dieet ter wereld' (Kosmos Uitgevers; Utrecht/Antwerpen, Netherlands), in Spanish as 'Plan DIOGENES para el control del peso. La dieta personalizada inteligente' (Editorial Evergráficas; León, Spain) and in English as 'World's Best Diet' (Penguin, Australia). The other authors have nothing to disclose.

Contributions:

We thank the Functional Biochemistry Facility for expert assistance with ELLA immunoassays.

AI and NVia designed and performed the network analyses; JM set up, optimized and supervised QuantSeq experiments, AC performed sequencing experiments, SM prepared and qc-ed RNA samples, JV performed RT-qPCR on full AT RNA samples and ThP1 cells, NB isolated AT cells and

extracted RNA, CL performed RT-qPCR on RNA of AT isolated cells, CM analyzed GDF15 plasma data, OW setup and directed NIHS biobank, GL helped with bioinformatics analyses, WHMS and AA: designed the DiOGenes clinical study, AV, NVig, WHMS, JH, and DL: designed the transcriptomics studies, AV and NVig directed and supervised the whole study, AI, NVia, NVig and AV performed all statistical analyses, interpreted the results and wrote the manuscript with input from all authors; AV and NVig had primary responsibility for the final content; and all authors read and approved the final manuscript.

Clinical Trial Identifier:

NCT00390637

GEO deposit:

GSE141221

Supplemental Material DOI:

10.6084/m9.figshare.12030486

Abstract

Context. Adipose tissue (AT) transcriptome studies provide holistic pictures of adaptation to weight and related bioclinical settings changes.

Objective. To implement AT gene expression profiling and investigate the link between changes in bioclinical parameters and AT gene expression during three steps of a two-phase dietary intervention (DI).

Design. AT transcriptome profiling was obtained from sequencing 1051 samples, corresponding to 556 distinct individuals enrolled in a weight loss intervention (8-week low calorie diet (LCD) at 800 kcal/d) followed with a 6-month *ad libitum* randomized DI.

Methods. Transcriptome profiles obtained with QuantSeq sequencing were benchmarked against Illumina RNAseq. RT-qPCR was used to further confirm associations. Cell specificity was assessed using freshly isolated cells and THP-1 cell line.

Results. During LCD, five modules were found, of which three included at least one bio-clinical variable. Change in BMI connected with changes in mRNA level of genes with inflammatory response signature. In this module, change in BMI was negatively associated to changes in expression of genes encoding secreted protein (*GDF15*, *CCL3* and *SPP1*).

Through all phases of the DI, change in *GDF15* was connected to changes in *SPP1*, *CCL3*, *LIPA* and *CD68*. Further characterization showed that these genes were specific to macrophages (with *LIPA*, *CD68* and *GDF15* expressed in anti-inflammatory macrophages) and *GDF15* also expressed in preadipocytes.

Conclusion. Network analyses identified a novel AT feature with *GDF15* upregulated with calorie restriction induced weight loss, concomitantly to macrophage markers. In AT, *GDF15* was expressed in preadipocytes and macrophages where it was a hallmark of anti-inflammatory cells.

Precis

A data driven approach in obese humans during and after calorie restriction revealed adipose tissue *GDF15* gene expression upregulated during weight loss with a cluster of macrophages genes.

1 Introduction

2 Combining biomarker and phenotypic data provides valuable opportunity to identify signatures of
3 diseases as well as response to treatments or lifestyle interventions, which may have implications for
4 understanding biology and clinical management (1–3).

5 Excess adiposity is associated to numerous comorbidities including metabolic complications such as
6 insulin resistance (IR), type 2 diabetes (T2D), and cardiovascular diseases (CVD) (4,5). Adipose tissue
7 (AT) is the main lipid storage organ of the human body. Through active secretory functions, it may
8 directly, or indirectly via cognate receptor, influence the activity of other metabolic organs such as
9 liver and skeletal muscle. AT secreted proteic factors, so-called adipocytokines are produced by
10 either adipocytes, precursor cells or resident AT macrophages. These cell types modify gene
11 expression in response to AT expansion or reduction. Furthermore, an AT dysfunction leads to an
12 altered secretory profile and is associated with increased inflammation and fibrosis (6). The plasticity
13 of AT during weight loss has been assessed by several gene expression studies, including
14 transcriptome-wide analyses (7) and targeted candidate approach (8). Yet, changes occurring
15 following weight loss and their link with weight regain still remain far from complete (9).

16 Additionally, very little is known about the relationship between weight regain, AT gene expression
17 changes, and other clinical readouts such as indices of insulin resistance, and markers of CVD. So far,
18 most studies have focused on pairwise assessment between a given transcript and a single clinical
19 readout. *De facto*, this limits our understanding of the physiological changes. Systems biology aims to
20 dissect complex relationships across the multiple scales of organization that characterize biological
21 systems (10,11). In particular, networks have proven useful to unravel the complex relations
22 (regulation, co-regulation) existing between gene expression profiles under various environmental
23 conditions (12). They are also a powerful approach to provide a global and comprehensive image of
24 the systems functioning related to complex traits by studying jointly multiple clinical parameters
25 (13,14).

26 In this study, we aim to characterize AT gene expression changes during a two-phase dietary
27 intervention in overweight and obese subjects using unsupervised and hypothesis-free methods. This
28 allowed us to identify modules of co-regulated genes related with clinical parameters pertaining to
29 weight regain, insulin-resistance and risk factors for developing CVD.

30

31 [Material and Methods](#)

32 [Ethics](#)

33 All studies were performed according to the latest version of the Declaration of Helsinki. Local ethics
34 committees approved all procedures that involved human participants and written informed consent
35 was obtained from all participants.

36 [Randomized dietary intervention study design](#)

37 The DiOGenes study (15) is a pan-European, multi-center, randomized controlled dietary intervention
38 program (NCT00390637). A CONSORT flowchart describing the intervention is shown in Figure 1A. In
39 this study, 938 overweight/obese, non-diabetic subjects followed a low-calorie diet (LCD) for eight
40 weeks using a meal replacement product (Modifast 800kcal/d, Nutrition et Santé, France). Subjects
41 achieving at least 8% of body weight loss were then included in a 6-month randomized dietary
42 intervention (DI) and were assigned to one of five *ad libitum* maintenance diets, consisting in low
43 protein/low glycaemic index, low protein /high glycaemic index, high protein/low glycaemic index,
44 high protein/ high glycaemic index, and control according to current national dietary guidelines.
45 Abdominal subcutaneous AT biopsies were obtained by needle aspiration, about 10 cm from the
46 umbilicus, under local anesthesia after an overnight fast. Plasma and AT samples were stored at -
47 80°C until processing. BMI, total plasma lipid levels, waist circumference and HOMA-IR were
48 obtained at baseline, upon weight loss and study termination. Lipid levels and HOMA-IR were
49 quantified following an overnight fast.

50

51 DiOGenes transcriptome analyses

52 Total RNA was extracted from AT samples as previously described (8). RNA samples were then
53 quantified with a fluorimetric method (Ribogreen, Thermo Fischer) and their integrity evaluated on a
54 fragment analyzer (Advanced Analytical). Good quality RNA was available for 471 individuals at
55 clinical investigation day (CID)1 (baseline), 330 at CID2 (at the end of the 8-w LCD) and 250 at CID3
56 (at the end of the 6-month DI) (Figure 1B). After sample randomization, 500 ng RNA was loaded on
57 multi-well plates, dried by vacuum concentration, and resuspended into 5 μ L nuclease free water.
58 Sequencing libraries covering the 3'-end of messenger RNA were prepared using the QuantSeq 3'
59 mRNA-Seq Library Prep Kit from Lexogen, strictly following the manufacturer's recommendations.
60 The optimal number of PCR cycles (15 cycles) was empirically evaluated by quantitative PCR. Libraries
61 were all quantified with a fluorimetric method (Picogreen, Thermo Fischer) and their size pattern
62 evaluated on a fragment analyzer (Advanced Analytical). Libraries were pooled equimolar by 96 and
63 clustered at a concentration of 9 pmol on 4 lanes of single read sequencing flow cells (Illumina).
64 Sequencing was performed for 65 cycles on a HiSeq 2500 (Illumina) using the SBS v4 chemistry
65 (Illumina).

66 After demultiplexing with bcl2fastq (standard parameters), sequencing reads were trimmed with
67 BBDuk (BBTools version 35.85, Bushnell B., sourceforge.net/projects/bbmap/) using the parameters
68 k=13, ktrim=r, forcetrimleft=11, mink=5, qtrim=t, trimq=10, minlength=20, rcomp=f, and providing
69 the sequence of the QuantSeq adaptors. Mapping to the human genome (built GRCh38.p2) was
70 performed with RNA STAR (16) (version 2.3.0e and using default parameters). Gene count was
71 performed with HTSeq (17) (version 0.5.4p3, with the parameters mode=intersection-nonempty,
72 stranded=yes, a= 10, and type=exon). The annotation file used was based on GENCODE (18) release
73 25 but was filtered for transcripts not classified as pseudogenes and with a transcript support level
74 "1" (for high quality annotation) or "NA" (for single exon transcripts). Only seven samples did not
75 reach the manufacturer's recommended criteria of 3M sequencing reads. Those samples were
76 reprocessed.

77 PCA was performed on log₂ transformed count data to identify possible outliers and batch effects.
78 This allowed to remove 3 atypical samples from the analysis (see Supplementary Figure S1). A second
79 PCA without these atypical samples allowed to identify a possible blood contamination in most
80 samples from UK. Samples with HBB larger than 20% (50 samples) were also removed from
81 subsequent analysis, together with a remaining outlier (see Supplementary Figure S2). In addition,
82 one plate with 79 samples had a higher variability than the other plates. Normalization was not able
83 to correct this plate-effect but differential analysis with and without the samples from this plate gave
84 very reproducible results (see Supplementary Figure S3). So we decided to remove the samples from
85 this plate from the analysis as well. This resulted in using 918 samples from 556 unique individuals in
86 the remaining of the analyses, distributed at the different time steps, as shown in Supplementary
87 Figure S4.

88

89 **Statistical analyses of QuantSeq data**

90 Unless specified otherwise, all statistical analyses were performed using R (version 3.4)(19). The overall
91 analysis strategy is summarized in Figure 2.

92 **Differential analysis** Pairwise time step analyses were performed to detect differentially expressed
93 genes between two CID (*i.e.*, contrasts: CID1 vs CID2, CID1 vs CID3 and CID2 vs CID3). For each
94 analysis, raw count data were normalized using the TMM approach (20) implemented in the R
95 package edgeR (21). Then, differentially expressed genes between the two conditions were extracted
96 using a Negative Binomial test with a fixed effect for the individual and a log ratio test. Multiple test
97 correction was performed with Benjamini-Hochberg (BH) False Discovery Rate (FDR)(22) within each
98 contrast and significance was set at FDR 5%. Genes whose expression was found equal to 0 in more
99 than 25% of the samples were removed from the analysis, as were genes whose expression was too
100 low in one condition, resulting in an impossible estimation of their fold change (FC). In addition, since
101 high dimensional data ($n < p$) would cause estimation issues for network inference methods, we

102 further restricted our list of differentially expressed genes to those having an absolute log fold-
103 change (FC) greater than $\log_2(1.3)$.

104 **Integration of clinical and transcriptome data** Associations between clinical variables (BMI, total
105 lipid levels, waist circumference and HOMA-IR) and gene expression were tested using linear mixed
106 effect models. Changes in gene expression (CPM \log_2 FC), gender and age were modelled as fixed
107 effects; the center was modelled as a random effect. Adjustment for multiple testing was performed
108 using BH correction.

109 **Network inference and mining** Similarly to (11), we performed a multi-step network inference to
110 obtain a comprehensive model of the overall interactions between gene expressions and clinical
111 variables. In such a model, nodes of the network correspond to genes or clinical variables and edges
112 correspond to strong and direct interactions between changes in gene expressions and/or clinical
113 variables between two-time steps.

114 Edges between genes and clinical variables were inferred using the aforementioned mixed effect
115 models. Edges between genes were inferred using the graphical Lasso (GLasso (23) as implemented in
116 the R package huge) on the \log_2 FC expression of differentially expressed genes for each contrast. Unlike
117 pairwise measure of associations, such as Pearson correlation coefficients, GLasso is based on partial
118 correlations and provides a stronger criterion for dependency by adjusting for common co-expressed
119 genes. This method is useful in order to filter out false positives by discovering only the most direct
120 interactions. Tuning of the GLasso regularization parameter was performed using the RIC criterion (see
121 Supplementary Methods). Finally, an unsupervised clustering of the nodes was performed for the
122 three networks using the modularity (24) optimization method of Reichardt et al. (25), as implemented
123 in the R package igraph (26). This led to obtain strongly connected groups of genes and/or clinical
124 variables for each network.

125 **Pathway analysis** The biological functions represented by genes in each module were searched using
126 Ingenuity Pathways Analysis (IPA) software version 7.5 (Ingenuity Systems, Redwood City, CA). Genes

127 for which IPA reported location as “Extracellular Space” were considered to encode secreted factors.
128 The significance of canonical pathways was tested using the Fisher Exact test with the User Dataset
129 of the 3 reference sets for each contrast.

130 **AT cell isolation**

131 The AT fractionation was performed as described in (27). Briefly, after collagenase digestion (250
132 U/mL in phosphate-buffered saline (PBS), 2% bovine serum albumin (BSA), pH 7.4, volume/volume)
133 of the AT for 30min at 37°C, the cell suspension was filtered through a 250 µm filter. The floating
134 mature adipocytes were collected, washed 3 times and stored at -80 °C. The remaining stroma
135 vascular fraction (SVF) was obtained after centrifugation. SVF cells were treated with erythrocyte
136 lysis buffer (155 mmol/L NH₄Cl; 5.7 mmol/L K₂HPO₄; 0.1 mmol/L EDTA; pH 7.3) followed by
137 successive filtrations through 100, 70, and 40 -µm strainers. The viable recovered cells were counted
138 and, after washing, the different SVF cells were isolated using an immunoselection/depletion
139 approach utilizing magnetic microbeads coupled to specific CD antibodies (CD31, CD34, CD14) which
140 are membrane cell markers to select the different SVF cell types. The preadipocytes are CD34-
141 positive cells (CD34+) and CD31-negative (CD31-) cells. The CD34-negative cells (CD34-) are immune
142 cells (macrophages which are also CD14+ cells and lymphocytes which are CD14- cells) as described
143 in (28). The cell extracts were collected and stored at -80°C until RNA extraction.

144 **THP-1 cell culture**

145 THP-1 cells were used as a human macrophage cell model. The cells were cultured in a humidified
146 incubator at 37 °C with 5% CO₂ in RPMI 1640 (Gibco) supplemented with 10% heat-inactivated FCS
147 (VWR) and 100 units/mL penicillin, 100 µg/mL streptomycin and 10mM HEPES (Gibco). Cells were
148 seeded at 5.5×10^5 cells/mL in 1 mL into 12 wells culture plates, then differentiated into M0
149 macrophage-like cells by stimulation with PMA 1 ng/mL (Sigma Aldrich) for four days followed by 48h
150 without PMA. To alter the phenotype, macrophages were primed for 48h with fresh medium
151 supplemented with LPS (2 ng/mL; Miltenyi Biotec) and IFN-γ (10 ng/mL; Miltenyi Biotec) to

152 differentiate into the M1-like phenotype, or IL-4 (20 ng/mL; Miltenyi Biotec) to the M2-like
153 phenotype. After washing, cell extracts were collected and stored at -80°C until RNA extraction.

154 Adipose tissue explants

155 AT explants were used for ex vivo studies. AT samples of about 400 mg obtained from needle
156 biopsies in 11 overweight (mean BMI 27.7 kg/m², SD 3.7) women aged 36.1 Y (SD 5.1) were cut into
157 small pieces and incubated for 4h in 4ml of Krebs/Ringer phosphate buffer supplemented with 1g/L
158 glucose and 20g/L BSA as described in (29).

159 RT-qPCR validation

160 Three hundred fifty-nine (359) individuals had good quality RNA at all 3 CIDs. The cDNA prepared
161 from 500 ng of total RNA and processed using the using Superscript II reverse transcriptase
162 (Invitrogen, St Aubin, France) in the presence of random hexamers were analyzed using the StepOne
163 Plus Real-Time PCR system (Applied Biosystems, Carlsbad, CA) and TaqMan assays (Applied
164 Biosystems) as described in Sramkova *et al* (29). The Taqman assays were obtained from Applied
165 Biosystems and the respective IDs were: *GDF15* (Hs00171132_m1), *SPP1* (Hs00959010_m1), *CD68*
166 (Hs00154355_m1), *LIPA* (Hs01548815_m1), *CCL3* (Hs00234142_m1), *PSMC4* (Hs00197826_m1),
167 *PUM1* (Hs01120030_m1), and *18S* (Hs99999901_s1). The relative gene expression was calculated as
168 $2^{-\Delta Ct}$ using *PUM1* as reference gene for full AT samples, *PSMC4* for THP1 cells or *18S* for AT isolated
169 cells data.

170 ELISA assays

171 GDF15 concentration in the buffer used for explants experiments was assessed using the ELLA
172 SinglePlex assays (ProteinSimple, San Jose, California, USA). Plasma protein levels of GDF15 were
173 measured in duplicate using human GDF15 ELISA kit (Human GDF-15 Quantikine ELISA Kit, Bio-
174 Techne), following manufacturer's instructions. The GDF15 concentrations were calculated using
175 sigmoidal standard curve fitted by nonlinear regression analysis for each test.

176 **Statistical analyses of RT-qPCR and ELISA data**

177 Gaussian distribution was tested using the D'Agostino & Pearson test. As data normality was not
178 fulfilled, comparison of expression distribution between groups was performed using Kruskal-Wallis
179 or Friedman test for unpaired or paired data respectively and Dunn's multiple comparison test.
180 Linear regression was performed with change in BMI as dependent variable.

181

182 **Results**

183

184 **Baseline characteristics and overall dietary intervention outcome**

185 In this report, we investigated gene expression changes within a subset of both men and women that
186 had followed a two-phase dietary intervention (see Methods and Figure 1A) and for which RNA
187 samples from AT biopsies were available (Figure 1B). At baseline, subjects were on average 41 years
188 old, with a mean BMI close to 35 kg/m² and a mean HOMA-IR at 2.93 (Table 1). Upon LCD, individuals
189 achieved, on average, 11% weight loss and upon study termination (6-months after weight loss)
190 10.8% weight loss. Both genders achieved similar weight loss relative to baseline (p=0.2376). These
191 characteristics are representative of all 918 enrolled subjects in the DiOGenes study.

192

193 **Differential gene expression analysis**

194 Upon quality control of the sequencing data (see Methods and Figure 1B), we assessed which genes
195 were differentially expressed between each paired clinical intervention time points (CID).

196 After filtering of low-quality genes, 6,290 genes were found differentially expressed for the contrast
197 CID1/2, 5,263 for the contrast CID1/3 and 4,461 for the contrast CID2/3. This resulted in a list of
198 9,156 unique genes that were found differentially expressed for at least one of the contrasts, among
199 which 1,228 were found differentially expressed for the three contrasts, as shown in Supplementary

200 Figure S5. Among these genes, 541 had an absolute log FC > $\log_2(1.3)$ for the contrast for CID1/2, 470
201 for the contrast CID1/3 and 661 for the contrast CID2/3 (for a total of 1,160 unique genes, used for
202 network inference as shown in Supplementary Figure S5). The list of expressed genes with results on
203 filtering and differential analysis can be found as supplementary material (Supplementary File S1).

204

205 **Replication with RNASeq data**

206 Taking advantage of previously generated RNAseq data for the CID1/2 contrast for 191 subjects (7),
207 we compared the RNAseq and QuantSeq technologies. Based on expression levels from 19,938
208 genes, we found a very strong correlation in expression fold-changes during LCD (Pearson $r^2=70\%$
209 with 95% CI [69.7%-71.2%], see Supplementary Figure S6A). Next, we attempted to replicate the 541
210 genes found differentially expressed with the QuantSeq analyses during LCD. At FDR 5%, 481 of those
211 genes replicated with RNAseq analysis (Supplementary Figure S6B), thereby demonstrating a 90%
212 replication rate between the two technologies.

213

214 **Network analyses reveal GDF15 as a novel partner in adipose tissue inflammation related genes**

215 We used a system biology approach to investigate the link between AT gene expression and clinical
216 parameters during a 2-phase DI including a LCD and the subsequent 6-month weight follow-up.

217 The first network analysis investigated the link between changes in AT gene expression and clinical
218 parameters during the LCD-induced weight loss phase (see Figure 3). The network was centered on a
219 clinical parameter, BMI, with both positive and negative relationship to a bunch of genes. Clustering
220 of the nodes (representing genes or clinical parameters with significant changes) of the graph was
221 performed. It revealed 5 modules with respectively 111, 89, 41, 131, and 131 nodes, with 3 of these
222 modules including at least one clinical parameter (See Supplementary File S2 for a full description of
223 the modules). Most of the modules contained more than 70% of down-regulated genes, except for

224 the module containing BMI that exhibited 89% of up-regulated genes. The lists of genes associated to
225 clinical variables in each module are displayed in the Supplementary File S3.

226 Pathway analyses of the genes were therefore performed for each module (supplementary Table S1).
227 Total cholesterol, LDL-cholesterol and HOMA-IR were included in the same module which contained
228 108 genes. “Cell development” and “lipid metabolism” were the top biological functions and
229 pathways represented. The changes in the mRNA level for 28 genes were positively connected to
230 changes in total cholesterol (and 6 genes with negative association). The change in LDL-cholesterol
231 was connected to change in mRNA level for 3 genes: *SSTR2* (positively), *U1* and *U1.1* (negatively).
232 These 3 genes were also connected to total cholesterol in the same manner. The lincRNA
233 *RP3.483K16.4* was the single gene connected, positively, to HOMA-IR. The module including waist
234 circumference contained 130 genes with 85% positively connected to waist circumference, indicating
235 that the highest was the reduction in waist circumference the greatest was the downregulation of
236 expression of these genes. “Lipid metabolism” was the top biological function represented. Four
237 genes encoded secreted proteins (*APOC4*, *EGFL6*, *SEMA3C*, *TNMD*). The BMI centered module
238 included 130 genes among which 80 were connected to BMI and, for 91%, with negative relationship
239 (Supplementary Figure S7A). “Inflammatory response” was the top biological function represented
240 with 51 genes. Fourteen genes encoded secreted factors (*CCL3*, *CHI3L1*, *CHIT1*, *FCGBP*, *FCGR3A*,
241 *FCMR*, *GDF15*, *IFI30*, *PILRA*, *PLA2G7*, *SDC4*, *SPP1*, *TREM2*, *ZG16B*), among which 12 were negatively
242 connected to BMI indicating that the highest was the decrease in BMI, the greatest was the up-
243 regulation of expression of these genes.

244 Our two subsequent network analyses investigated changes during the weight follow-up (CID2/3)
245 and the overall DI (CID1/3). We identified 7 modules (with size 20-83 nodes) for CID1/3 and 8
246 modules (size 6-142) for CID2/3 (see details in Supplementary File S2). Both networks exhibited a
247 module containing BMI as biological variable. For each contrast, the biological functions represented
248 in the modules with BMI were “organismal injuries” and “lipid metabolism” (supplementary Table

249 S1). The “lipid metabolism” pathway was representative of the module containing HDL for CID2/3.
250 Regarding these two contrasts (CID1/3 and CID2/3), the modules containing the BMI were composed
251 of genes representing different biological functions (lipid metabolism and organismal injuries,
252 respectively). Also, both networks contained a module with a cluster of co-regulated genes
253 composed of *CCL3*, *CD68*, *GDF15*, *LIPA*, and *SPP1* (Supplementary Figures S7B and S7C).
254 The cluster was also found in the module containing BMI from the LCD-induced weight loss phase
255 (Supplementary Figure S7A). This observation led us to focus on *GDF15* which was recently reported
256 as a nutritional stress marker (30), and the four other genes of the cluster (*CCL3*, *CD68*, *LIPA*, and
257 *SPP1*) which are markers for AT macrophages (31).

258

259 **Validation using RT-qPCR**

260 Validation of findings used RT-qPCR and a larger subset of the DiOGenes study (590 individuals, 116
261 men and 474 women at baseline, including 352 individuals with paired samples regarding all
262 contrasts).

263 The negative association between the change in AT *GDF15* gene expression and the change in BMI
264 was confirmed during LCD (contrast CID1/2). A low positive association was found during weight
265 follow-up, but not across the whole dietary intervention (Supplementary Figure S8).

266 All five genes of the cluster of macrophage markers had relative expression significantly different
267 between all pairwise time-contrasts (and with FDR adjusted p-values < 0.05). Notably all genes
268 marked a strong up-regulation during LCD, followed with a down-regulation during the following 6-
269 month weight control phase and with expression levels significantly lower than their baseline levels
270 (Figure 4).

271 Reports of GDF15 in AT are scarce, and none describe the cell type of origin. Therefore, we compared
272 *GDF15* expression between isolated adipocytes and stroma vascular cells isolated from human AT
273 together with gene expression of *CCL3*, *CD68*, *LIPA*, and *SPP1*.

274 Compared to isolated adipocytes, *GDF15* mRNA levels were higher in the stromal fraction, mainly in
275 pre-adipocytes and macrophages (Figure 5). The four other genes were predominantly expressed in
276 macrophages.

277 We next investigated the expression profile of these 5 genes according to phenotypic profile of the
278 human macrophages cell line THP-1. Once induced to M0 macrophages, the THP-1 cells were
279 polarized to M1-like (pro-inflammatory) or M2-like (anti-inflammatory) phenotype. All genes
280 exhibited differential expression between M1 and M2 THP-1 cells, with *CD68*, *GDF15*, and *LIPA*
281 having higher expression in M2 than M1 macrophages, while *CCL3* and *SPP1* mRNA levels were
282 higher in M1 cells (Figure 6).

283

284 **Analyses of GDF15 protein**

285 Next, we sought to confirm the observed AT *GDF15* mRNA levels at the protein levels in AT and
286 blood. The secretion of GDF15 by AT was assessed using subcutaneous AT explants from 11
287 overweight women. GDF15 concentration in the media from the AT explants was 440.9 ± 114.2
288 pg/mL (mean \pm SD, data not shown). Changes in circulating GDF15 was investigated in a subset of 28
289 individuals with both plasma samples, clinical and AT RT-qPCR data available at all CIDs. At baseline
290 plasma GDF15 was 473.5 ± 184.9 pg/mL. No significant change in plasma GDF15 was found across all
291 phases of the dietary intervention ($p = 0.4908$, Supplementary Figure S9A). A positive association
292 between plasma GDF15 and *GDF15* gene expression in adipose tissue was observed at baseline
293 (Supplementary Figure S9B), but no correlation between change in AT *GDF15* expression and
294 variations in plasma concentrations was found (p -value > 0.5). The negative association between
295 change in plasma GDF15 and change in BMI during the LCD was previously reported (32), but no

296 significant association was found during weight follow-up or across the whole DI (p-value > 0.4) (data
297 not shown).

298

299 Discussion

300 In this study, we investigated gene expression changes in AT, during a two-phase dietary intervention
301 in overweight/obese, non-diabetic subjects. Our systems biology approach enables to relate such
302 changes with changes in different clinical parameters associated to obesity or comorbidities (BMI,
303 waist circumference, total lipid levels, and HOMA-IR). In a discovery phase, we implemented the
304 QuantSeq technology (33) that enables to substantially reduce the sequencing costs (by about 5x
305 only in term of reagent costs), while keeping high-quality transcriptomic profiling for all Human
306 protein-coding genes. This allowed us to assess a large RNA collection (>1,000 samples stemming
307 from a clinical intervention). Re-analysis with nearly 400 samples using Illumina RNASeq
308 demonstrated a 90% replication rate. Also, our validation phase, using RT-qPCR in >1,000 samples
309 further reproduced our initial findings, thereby validating the QuantSeq technology.

310 Through a network-based approach, we identified BMI as a key node, indicating that this specific
311 clinical outcome has a major link with gene expression. Also, there was one specific transcriptomic
312 cluster including the *GDF15* gene, whose expression change during weight loss was linked with BMI
313 change. Of note, *GDF15* was not identified in previous differential gene expression analyses following
314 LCD-induced weight loss (7). *GDF15* (growth differentiation factor 15)/MIC-1 (macrophage inhibitory
315 cytokine-1)/NAG-1 (nonsteroidal anti-inflammatory drug-activated gene) is a member of the
316 transforming growth factor β (TGF- β) superfamily, that was first identified as a blocker of
317 macrophage activation (34). Its expression is ubiquitous and circulating concentration range is high
318 (35). Recently, *GDF15* has generated considerable attention in the field of obesity and weight
319 control. Notably, targeting *GDF15* for the treatment of obesity and anorexia is the subject of several
320 studies (35–40).

321 Preclinical studies in mice showed that GDF15 suppresses food intake (41) and recombinant GDF15
322 administration lowers body weight (42). Also, GDF15 can directly increase thermogenesis and
323 improve insulin sensitivity (43). In human, a rise in blood levels was reported with acute
324 exercise (32,44) and exercise training (45). Regarding weight loss, during or after termination of
325 calorie restriction, an increase was observed in obese individuals upon bariatric surgery (46), and 2
326 weeks metformin-induced weight loss (47). Small-scale dietary studies also showed no (PMID:
327 32020057 DOI: 10.1038/s41430-020-0568-9) or slight increase in plasma GDF15 following light or
328 drastic calorie restriction, for 48h or over 28 days (30). This was also confirmed in serum upon very-
329 low calorie diet (48). In addition, T2D patients exhibited lower GDF15 plasma levels 6 months after
330 the termination of an 8-week very-low calorie diet (PMID: 33925808 PMCID: PMC8146720 DOI:
331 10.3390/nu13051465). Hence, circulating GDF15 is considered as a nutritional stress marker (30).

332 Only few studies investigated the ATs (51,52). In our study, we found that GDF15 is released by AT
333 and *GDF15* gene expression in AT was up-regulated upon an 8-week low calorie diet, in association
334 with change in BMI and independently of change in plasma lipid profile or insulin resistance. The
335 baseline plasma level was in range with other studies (37). No significant change was found in plasma
336 ($p>0.4$). This might be due to the low power of the plasma study (only 28 individuals were
337 investigated), or a low contribution of AT to circulating GDF15 compared to other tissues, as
338 suggested by the lack of association between changes in AT *GDF15* expression and variations in
339 circulating GDF15. In AT, we noticed that the *GDF15* up-regulation was only transient, as *GDF15* gene
340 expression levels were significantly reduced in the 6-month following the acute weight loss phase
341 despite sustained weight loss, compared to baseline. Importantly, AT *GDF15* mRNA levels were
342 significantly reduced at study termination compared to baseline. However, plasma GDF15 remained
343 steady. This indicates that AT *GDF15* upregulation is induced by a negative energy balance. Also, it
344 tends to suggest that this is linked to AT remodeling during LCD, and that upon the acute weight loss
345 phase, the metabolic improvements (both in term of weight loss and insulin sensitivity) relates to

346 generally higher GDF15 levels. It is to be noticed that GDF15 induces lipolysis as recently reported
347 (32).

348 The identification of GDF15 as a factor released by the AT led to the observation that this adipokine
349 is produced by both adipocytes and stromal cells, with higher *GDF15* expression in subcutaneous
350 than visceral AT and expression negatively associated with body fat mass in both fat depots (51). In
351 human AT, *GDF15* expression was reported as a marker of oxidative stress negatively associated to
352 lipogenic gene markers (52). In the present study, changes in *GDF15* mRNA levels are positively
353 associated with changes in expression of macrophages markers (*CCL3*, *CD68*, *LIPA*, *SPP1*) in all
354 contrasts. We show that *GDF15* expression arises from two human AT cell types, preadipocytes and
355 macrophages, while expression of the four genes (*CCL3*, *CD68*, *LIPA* and *SPP1*), all co-expressed with
356 *GDF15*, only displayed macrophages-specific profiles. Macrophages exhibit phenotypic heterogeneity
357 and plasticity, depending on their microenvironment. These cells originate from circulating
358 monocytes and infiltrate tissues where they play various functions including tissue cleanup and
359 repair. The M1 and M2 classification is an oversimplification of a continuum in activation states, and
360 individual markers may fail to specify such polarization phenotype (53). M1-like macrophages
361 promote AT inflammation and insulin resistance; while M2 macrophages have an anti-inflammatory
362 role (54). We found that *GDF15* was more expressed in M2-like macrophages. This is consistent with
363 a mice study showing that *GDF15* expression was previously reported suppressed in M1-like
364 macrophages (55). *GDF15* also enhances the oxidative function of macrophages, leading to
365 polarization into an M2-like phenotype (55). Interestingly our data show that preadipocytes which
366 are part of the SVF cells, and not differentiated adipocytes, also express *GDF15* at similar level than
367 macrophages. While preadipocytes *GDF15* expression studies remain scarce (52,56), these cells can
368 be reprogrammed through dietary-induced weight loss and contribute to improvement of the
369 metabolic syndrome (57). Further studies are needed to elucidate the potential contribution of
370 preadipocytes to weight loss and related metabolic dysfunction improvements through *GDF15*
371 expression.

372 We also report different expression profiles of the macrophage markers associated to *GDF15*. *SPP1*
373 and *CCL3* expression levels were higher in M1-like macrophages. Osteopontin, encoded by *SPP1*, is
374 an important component of immune response and inflammation (58). *SPP1* expression is positively
375 associated to AT macrophages accumulation (59), and osteopontin plays a role in the development of
376 insulin resistance (60). *CCL3* encodes MIP-1 α , a member of the CC chemokine family that is produced
377 by a variety of cells, including resident and recruited macrophages (61). Conversely, *LIPA* and *CD68*
378 expression levels were higher in M2-like macrophages. *LIPA*, encodes the lysosomal acid lipase
379 protein that breaks down cholesteryl esters and triglycerides in human macrophages. Its expression
380 and activity have been reported to be decreased in the metabolic syndrome (62). *CD68* encodes a
381 membrane protein marker and in our analyses, we observed its expression in both M1 and M2
382 macrophages (with slightly higher levels in the latter population). This is consistent with previous
383 reports on CD68, that document it as a general marker of macrophages, whose expression is directly
384 linked with the number of macrophages, and that associates with both pro- and anti-inflammatory
385 markers (63).

386 In obese individuals, weight loss induces a decrease in pro-inflammatory and an increase in anti-
387 inflammatory factors (64). The up-regulation of these five genes during LCD may be a hallmark of the
388 beneficial effect of calorie restriction-induced weight loss on AT inflammation. Lending support to
389 this hypothesis, a recent study showed that treatment of obese mice with GDF15 improves the
390 oxidative function of AT macrophages and reverses insulin resistance (55). As no significant change in
391 circulating GDF15 was found, the present study indicates a paracrine/autocrine role of GDF15 within
392 AT. The study cannot provide evidence on whether the enhanced GDF15 expression during LCD
393 originates from preadipocytes or macrophages, however, a strong co-regulation of both M1 and M2
394 macrophages markers was found. GDF15 appears as an anti-inflammatory marker. In addition to the
395 decrease in the anti-lipolytic insulin, the pro-lipolytic GDF15 locally produced within AT may
396 contribute to LCD-induced weight loss (32). The fatty acids produced by adipocytes could thereby
397 induce transient local inflammation.

398 In summary, we identified an AT signature as a cluster of macrophage-related genes, through a
399 transcriptome-wide systems biology approach. Specifically, a module including *GDF15* was identified;
400 while *GDF15* is currently the focus of targeted studies, it demonstrates the validity of our approach
401 to identify potentially relevant biomarkers of clinical improvements during dietary intervention. And
402 indeed, our approach highlighted a novel macrophage signature composed of genes co-regulated
403 with *GDF15*.

References

1. **Leon-Mimila P, Wang J, Huertas-Vazquez A.** Relevance of Multi-Omics Studies in Cardiovascular Diseases. *Front Cardiovasc Med* 2019;6. doi:10.3389/fcvm.2019.00091.
2. **Valsesia A, Saris WH, Astrup A, Hager J, Masoodi M.** Distinct lipid profiles predict improved glycemic control in obese, nondiabetic patients after a low-caloric diet intervention: the Diet, Obesity and Genes randomized trial. *Am J Clin Nutr* 2016;104(3):566–575.
3. **Musaad S, Haynes EN.** Biomarkers of Obesity and Subsequent Cardiovascular Events. *Epidemiol Rev* 2007;29:98–114.
4. **Dixon JB.** The effect of obesity on health outcomes. *Mol. Cell. Endocrinol.* 2010;316(2):104–108.
5. **Haslam DW, James WPT.** Obesity. *Lancet* 2005;366(9492):1197–1209.
6. **Vegiopoulos A, Rohm M, Herzig S.** Adipose tissue: between the extremes. *EMBO J.* 2017;36(14):1999–2017.
7. **Armenise C, Lefebvre G, Carayol J, Bonnel S, Bolton J, Di Cara A, Gheldof N, Descombes P, Langin D, Saris WH, Astrup A, Hager J, Viguerie N, Valsesia A.** Transcriptome profiling from adipose tissue during a low-calorie diet reveals predictors of weight and glycemic outcomes in obese, nondiabetic subjects. *Am J Clin Nutr* 2017;106(3):736–746.
8. **Viguerie N, Montastier E, Maoret J-J, Roussel B, Combes M, Valle C, Villa-Vialaneix N, Iacovoni JS, Martinez JA, Holst C, Astrup A, Vidal H, Clément K, Hager J, Saris WHM, Langin D.** Determinants of Human Adipose Tissue Gene Expression: Impact of Diet, Sex, Metabolic Status, and Cis Genetic Regulation. *PLoS Genet* 2012;8(9):e1002959.
9. **Bolton J, Montastier E, Carayol J, Bonnel S, Mir L, Marques M-A, Astrup A, Saris W, Iacovoni J, Villa-Vialaneix N, Valsesia A, Langin D, Viguerie N.** Molecular Biomarkers for Weight Control in Obese Individuals Subjected to a Multiphase Dietary Intervention. *J Clin Endocrinol Metab* 2017;102(8):2751–2761.
10. **De Smet R, Marchal K.** Advantages and limitations of current network inference methods. *Nature Reviews Microbiology* 2010;8(10):717–729.
11. **Montastier E, Villa-Vialaneix N, Caspar-Bauguil S, Hlavaty P, Tvrzicka E, Gonzalez I, Saris WHM, Langin D, Kunesova M, Viguerie N.** System model network for adipose tissue signatures related to weight changes in response to calorie restriction and subsequent weight maintenance. *PLoS Comput. Biol.* 2015;11(1):e1004047.
12. **Civelek M, Lusis AJ.** Systems genetics approaches to understand complex traits. *Nat. Rev. Genet.* 2014;15(1):34–48.
13. **Peters LA, Perrigoue J, Mortha A, Iuga A, Song W, Neiman EM, Llewellyn SR, Di Narzo A, Kidd BA, Telesco SE, Zhao Y, Stojmirovic A, Sendekci J, Shameer K, Miotto R, Losic B, Shah H, Lee E, Wang M, Faith JJ, Kasarskis A, Brodmerkel C, Curran M, Das A, Friedman JR, Fukui Y, Humphrey MB, Iritani BM, Sibinga N, Tarrant TK, Argmann C, Hao K, Roussos P, Zhu J, Zhang B, Dobrin R, Mayer LF, Schadt EE.** A functional genomics predictive network model identifies regulators of inflammatory bowel disease. *Nat Genet* 2017;49(10):1437–1449.

14. **Le TT, Savitz J, Suzuki H, Misaki M, Teague TK, White BC, Marino JH, Wiley G, Gaffney PM, Drevets WC, McKinney BA, Bodurka J.** Identification and replication of RNA-Seq gene network modules associated with depression severity. *Translational Psychiatry* 2018;8(1):180.
15. **Larsen TM, Dalskov S-M, van Baak M, Jebb SA, Papadaki A, Pfeiffer AFH, Martinez JA, Handjieva-Darlenska T, Kunešová M, Pihlsgård M, Stender S, Holst C, Saris WHM, Astrup A, Diet, Obesity, and Genes (Diogenes) Project.** Diets with high or low protein content and glycemic index for weight-loss maintenance. *N. Engl. J. Med.* 2010;363(22):2102–2113.
16. **Dobin A, Davis CA, Schlesinger F, Drenkow J, Zaleski C, Jha S, Batut P, Chaisson M, Gingeras TR.** STAR: ultrafast universal RNA-seq aligner. *Bioinformatics* 2013;29(1):15–21.
17. **Anders S, Pyl PT, Huber W.** HTSeq - A Python framework to work with high-throughput sequencing data. *Bioinformatics* 2015;31. doi:10.1093/bioinformatics/btu638.
18. **Frankish A, Diekhans M, Ferreira A-M, Johnson R, Jungreis I, Loveland J, Mudge JM, Sisu C, Wright J, Armstrong J, Barnes I, Berry A, Bignell A, Carbonell Sala S, Chrast J, Cunningham F, Di Domenico T, Donaldson S, Fiddes IT, García Girón C, Gonzalez JM, Grego T, Hardy M, Hourlier T, Hunt T, Izuogu OG, Lagarde J, Martin FJ, Martínez L, Mohanan S, Muir P, Navarro FCP, Parker A, Pei B, Pozo F, Ruffier M, Schmitt BM, Stapleton E, Suner M-M, Sycheva I, Uszczyńska-Ratajczak B, Xu J, Yates A, Zerbino D, Zhang Y, Aken B, Choudhary JS, Gerstein M, Guigó R, Hubbard TJP, Kellis M, Paten B, Reymond A, Tress ML, Flicek P.** GENCODE reference annotation for the human and mouse genomes. *Nucleic Acids Res.* 2019;47(D1):D766–D773.
19. **R Core Team.** *R: A Language and Environment for Statistical Computing.* Vienna, Austria: R Foundation for Statistical Computing; 2017. Available at: <http://www.R-project.org>.
20. **Robinson MD, Oshlack A.** A scaling normalization method for differential expression analysis of RNA-seq data. *Genome Biology* 2010;11(3):R25.
21. **Robinson MD, McCarthy DJ, Smyth GK.** edgeR: a Bioconductor package for differential expression analysis of digital gene expression data. *Bioinformatics* 2009;26. doi:10.1093/bioinformatics/btp616.
22. **Benjamini Y, Hochberg Y.** Controlling the False Discovery Rate: A Practical and Powerful Approach to Multiple Testing. *Journal of the Royal Statistical Society. Series B (Methodological)* 1995;57(1):289–300.
23. **Friedman J, Hastie T, Tibshirani R.** Sparse inverse covariance estimation with the graphical lasso. *Biostatistics* 2008;9(3):432–441.
24. **Newman MEJ, Girvan M.** Finding and evaluating community structure in networks. *Phys. Rev. E* 2004;69(2):026113.
25. **Reichardt J, Bornholdt S.** Statistical mechanics of community detection. *Phys. Rev. E* 2006;74(1):016110.
26. **Csardi G, Nepusz T.** The igraph software package for complex network research. *InterJournal* 2006;Complex Systems:1695.
27. **Curat CA, Miranville A, Sengenès C, Diehl M, Tonus C, Busse R, Bouloumié A.** From blood monocytes to adipose tissue-resident macrophages: induction of diapedesis by human mature adipocytes. *Diabetes* 2004;53(5):1285–1292.

28. **Maumus M, Peyrafitte J-A, D'Angelo R, Fournier-Wirth C, Bouloumié A, Casteilla L, Sengenès C, Bourin P.** Native human adipose stromal cells: localization, morphology and phenotype. *Int J Obes (Lond)* 2011;35(9):1141–1153.
29. **Sramkova V, Berend S, Siklova M, Caspar-Bauguil S, Carayol J, Bonnel S, Marques M, Decaunes P, Kolditz C-I, Dahlman I, Arner P, Stich V, Saris WHM, Astrup A, Valsesia A, Rossmeislova L, Langin D, Viguerie N.** Apolipoprotein M: a novel adipokine decreasing with obesity and upregulated by calorie restriction. *Am J Clin Nutr.* doi:10.1093/ajcn/nqy331.
30. **Patel S, Alvarez-Guaita A, Melvin A, Rimmington D, Dattilo A, Miedzybrodzka EL, Cimino I, Maurin A-C, Roberts GP, Meek CL, Virtue S, Sparks LM, Parsons SA, Redman LM, Bray GA, Liou AP, Woods RM, Parry SA, Jeppesen PB, Kolnes AJ, Harding HP, Ron D, Vidal-Puig A, Reimann F, Gribble FM, Hulston CJ, Farooqi IS, Fafournoux P, Smith SR, Jensen J, Breen D, Wu Z, Zhang BB, Coll AP, Savage DB, O'Rahilly S.** GDF15 Provides an Endocrine Signal of Nutritional Stress in Mice and Humans. *Cell Metabolism* 2019;29(3):707-718.e8.
31. **Klimcakova E, Roussel B, Kovacova Z, Kovacikova M, Siklova-Vitkova M, Combes M, Hejnova J, Decaunes P, Maoret JJ, Vedral T, Viguerie N, Bourlier V, Bouloumié A, Stich V, Langin D.** Macrophage gene expression is related to obesity and the metabolic syndrome in human subcutaneous fat as well as in visceral fat. *Diabetologia* 2011;54(4):876–887.
32. **Laurens C, Parmar A, Murphy E, Carper D, Lair B, Maes P, Vion J, Boulet N, Fontaine C, Marqués M-A, Larrouy D, Harant I, Thalamas C, Montastier E, Caspar-Bauguil S, Bourlier V, Tavernier G, Grolleau J-L, Bouloumié A, Langin D, Viguerie N, Bertile F, Blanc S, de Glisezinski I, O'Gorman DJ, Moro C.** Growth and Differentiation Factor 15 is secreted by skeletal muscle during exercise and promotes lipolysis in humans. *JCI Insight* 2020. doi:10.1172/jci.insight.131870.
33. **Moll P, Ante M, Seitz A, Reda T.** QuantSeq 3' mRNA sequencing for RNA quantification. *Nature Methods* 2014;11:972.
34. **Bootcov MR, Bauskin AR, Valenzuela SM, Moore AG, Bansal M, He XY, Zhang HP, Donnellan M, Mahler S, Pryor K, Walsh BJ, Nicholson RC, Fairlie WD, Por SB, Robbins JM, Breit SN.** MIC-1, a novel macrophage inhibitory cytokine, is a divergent member of the TGF-beta superfamily. *Proc Natl Acad Sci U S A* 1997;94(21):11514–11519.
35. **Mullican SE, Rangwala SM.** Uniting GDF15 and GFRAL: Therapeutic Opportunities in Obesity and Beyond. *Trends Endocrinol. Metab.* 2018;29(8):560–570.
36. **Frikke-Schmidt H, Hultman K, Galaske JW, Jørgensen SB, Myers MG, Seeley RJ.** GDF15 acts synergistically with liraglutide but is not necessary for the weight loss induced by bariatric surgery in mice. *Mol Metab* 2019;21:13–21.
37. **Mullican SE, Lin-Schmidt X, Chin C-N, Chavez JA, Furman JL, Armstrong AA, Beck SC, South VJ, Dinh TQ, Cash-Mason TD, Cavanaugh CR, Nelson S, Huang C, Hunter MJ, Rangwala SM.** GFRAL is the receptor for GDF15 and the ligand promotes weight loss in mice and nonhuman primates. *Nat. Med.* 2017;23(10):1150–1157.
38. **Yang L, Chang C-C, Sun Z, Madsen D, Zhu H, Padkjær SB, Wu X, Huang T, Hultman K, Paulsen SJ, Wang J, Bugge A, Frantzen JB, Nørgaard P, Jeppesen JF, Yang Z, Secher A, Chen H, Li X, John LM, Shan B, He Z, Gao X, Su J, Hansen KT, Yang W, Jørgensen SB.** GFRAL is the receptor for GDF15 and is required for the anti-obesity effects of the ligand. *Nat. Med.* 2017;23(10):1158–1166.

39. **Hsu J-Y, Crawley S, Chen M, Ayupova DA, Lindhout DA, Higbee J, Kutach A, Joo W, Gao Z, Fu D, To C, Mondal K, Li B, Kekatpure A, Wang M, Laird T, Horner G, Chan J, McEntee M, Lopez M, Lakshminarasimhan D, White A, Wang S-P, Yao J, Yie J, Matern H, Solloway M, Haldankar R, Parsons T, Tang J, Shen WD, Alice Chen Y, Tian H, Allan BB.** Non-homeostatic body weight regulation through a brainstem-restricted receptor for GDF15. *Nature* 2017;550(7675):255–259.
40. **Emmerson PJ, Wang F, Du Y, Liu Q, Pickard RT, Gonciarz MD, Coskun T, Hamang MJ, Sindelar DK, Ballman KK, Foltz LA, Muppidi A, Alsina-Fernandez J, Barnard GC, Tang JX, Liu X, Mao X, Siegel R, Sloan JH, Mitchell PJ, Zhang BB, Gimeno RE, Shan B, Wu X.** The metabolic effects of GDF15 are mediated by the orphan receptor GFRAL. *Nat. Med.* 2017;23(10):1215–1219.
41. **Johnen H, Lin S, Kuffner T, Brown DA, Tsai VW-W, Bauskin AR, Wu L, Pankhurst G, Jiang L, Junankar S, Hunter M, Fairlie WD, Lee NJ, Enriquez RF, Baldock PA, Corey E, Apple FS, Murakami MM, Lin E-J, Wang C, During MJ, Sainsbury A, Herzog H, Breit SN.** Tumor-induced anorexia and weight loss are mediated by the TGF-beta superfamily cytokine MIC-1. *Nat. Med.* 2007;13(11):1333–1340.
42. **Tsai VWW, Husaini Y, Sainsbury A, Brown DA, Breit SN.** The MIC-1/GDF15-GFRAL Pathway in Energy Homeostasis: Implications for Obesity, Cachexia, and Other Associated Diseases. *Cell Metab.* 2018;28(3):353–368.
43. **Tsai VW, Zhang HP, Manandhar R, Lee-Ng KKM, Lebhar H, Marquis CP, Husaini Y, Sainsbury A, Brown DA, Breit SN.** Treatment with the TGF-b superfamily cytokine MIC-1/GDF15 reduces the adiposity and corrects the metabolic dysfunction of mice with diet-induced obesity. *Int J Obes (Lond)* 2018;42(3):561–571.
44. **Kleinert M, Clemmensen C, Sjøberg KA, Carl CS, Jeppesen JF, Wojtaszewski JFP, Kiens B, Richter EA.** Exercise increases circulating GDF15 in humans. *Mol Metab* 2018;9:187–191.
45. **Zhang H, Fealy CE, Kirwan JP.** Exercise training promotes a GDF15-associated reduction in fat mass in older adults with obesity. *Am. J. Physiol. Endocrinol. Metab.* 2019;316(5):E829–E836.
46. **Kleinert M, Bojsen-Møller KN, Jørgensen NB, Svane MS, Martinussen C, Kiens B, Wojtaszewski JFP, Madsbad S, Richter EA, Clemmensen C.** Effect of bariatric surgery on plasma GDF15 in humans. *Am. J. Physiol. Endocrinol. Metab.* 2019;316(4):E615–E621.
47. **Coll AP, Chen M, Taskar P, Rimmington D, Patel S, Tadross JA, Cimino I, Yang M, Welsh P, Virtue S, Goldspink DA, Miedzybrodzka EL, Konopka AR, Esponda RR, Huang JT-J, Tung YCL, Rodriguez-Cuenca S, Tomaz RA, Harding HP, Melvin A, Yeo GSH, Preiss D, Vidal-Puig A, Vallier L, Nair KS, Wareham NJ, Ron D, Gribble FM, Reimann F, Sattar N, Savage DB, Allan BB, O’Rahilly S.** GDF15 mediates the effects of metformin on body weight and energy balance. *Nature* 2020;578(7795):444–448.
48. **Dostálová I, Roubíček T, Bártlová M, Mráz M, Lacinová Z, Haluzíková D, Kaválková P, Matoulek M, Kasalický M, Haluzík M.** Increased serum concentrations of macrophage inhibitory cytokine-1 in patients with obesity and type 2 diabetes mellitus: the influence of very low calorie diet. *European Journal of Endocrinology* 2009;161(3):397–404.
51. **Ding Q, Mracek T, Gonzalez-Muniesa P, Kos K, Wilding J, Trayhurn P, Bing C.** Identification of macrophage inhibitory cytokine-1 in adipose tissue and its secretion as an adipokine by human adipocytes. *Endocrinology* 2009;150(4):1688–1696.

52. Šrámková V, Koc M, Krauzová E, Kračmerová J, Šiklová M, Elkalaf M, Langin D, Štich V, Rossmeislová L. Expression of lipogenic markers is decreased in subcutaneous adipose tissue and adipocytes of older women and is negatively linked to GDF15 expression. *J. Physiol. Biochem.* 2019;75(3):253–262.
53. Martinez FO, Gordon S. The evolution of our understanding of macrophages and translation of findings toward the clinic. *Expert Rev Clin Immunol* 2015;11(1):5–13.
54. Appari M, Channon KM, McNeill E. Metabolic Regulation of Adipose Tissue Macrophage Function in Obesity and Diabetes. *Antioxid. Redox Signal.* 2018;29(3):297–312.
55. Jung S-B, Choi MJ, Ryu D, Yi H-S, Lee SE, Chang JY, Chung HK, Kim YK, Kang SG, Lee JH, Kim KS, Kim HJ, Kim C-S, Lee C-H, Williams RW, Kim H, Lee HK, Auwerx J, Shong M. Reduced oxidative capacity in macrophages results in systemic insulin resistance. *Nat Commun* 2018;9(1):1551.
56. Yanagitai M, Kitagawa T, Okawa K, Koyama H, Satoh T. Phenylenediamine derivatives induce GDF-15/MIC-1 and inhibit adipocyte differentiation of mouse 3T3-L1 cells. *Biochem. Biophys. Res. Commun.* 2012;417(1):294–298.
57. Rossmeislová L, Mališová L, Kračmerová J, Tencerová M, Kováčová Z, Koc M, Šiklová-Vítková M, Viquerie N, Langin D, Štich V. Weight Loss Improves the Adipogenic Capacity of Human Preadipocytes and Modulates Their Secretory Profile. *Diabetes* 2013;62(6):1990–1995.
58. Kahles F, Findeisen HM, Bruemmer D. Osteopontin: A novel regulator at the cross roads of inflammation, obesity and diabetes. *Mol Metab* 2014;3(4):384–393.
59. Bertola A, Deveaux V, Bonnafous S, Rousseau D, Anty R, Wakkach A, Dahman M, Tordjman J, Clément K, McQuaid SE, Frayn KN, Huet P-M, Gugenheim J, Lotersztajn S, Le Marchand-Brustel Y, Tran A, Gual P. Elevated expression of osteopontin may be related to adipose tissue macrophage accumulation and liver steatosis in morbid obesity. *Diabetes* 2009;58(1):125–133.
60. Kiefer FW, Zeyda M, Todoric J, Huber J, Geyeregger R, Weichhart T, Aszmann O, Ludvik B, Silberhumer GR, Prager G, Stulnig TM. Osteopontin expression in human and murine obesity: extensive local up-regulation in adipose tissue but minimal systemic alterations. *Endocrinology* 2008;149(3):1350–1357.
61. Hill AA, Reid Bolus W, Hasty AH. A decade of progress in adipose tissue macrophage biology. *Immunol. Rev.* 2014;262(1):134–152.
62. Lin E, Kuo P-H, Liu Y-L, Yang AC, Kao C-F, Tsai S-J. Association and interaction of APOA5, BUD13, CETP, LIPA and health-related behavior with metabolic syndrome in a Taiwanese population. *Sci Rep* 2016;6:36830.
63. Fjeldborg K, Pedersen SB, Møller HJ, Christiansen T, Bennetzen M, Richelsen B. Human Adipose Tissue Macrophages Are Enhanced but Changed to an Anti-Inflammatory Profile in Obesity. *Journal of Immunology Research* 2014. doi:10.1155/2014/309548.
64. Canello R, Henegar C, Viquerie N, Taleb S, Poitou C, Rouault C, Coupaye M, Pelloux V, Hugol D, Bouillot J-L, Bouloumié A, Barbatelli G, Cinti S, Svensson P-A, Barsh GS, Zucker J-D, Basdevant A, Langin D, Clément K. Reduction of macrophage infiltration and chemoattractant gene expression changes in white adipose tissue of morbidly obese subjects after surgery-induced weight loss. *Diabetes* 2005;54(8):2277–2286.

Legends for Figures

Figure 1: Flowcharts of dietary intervention and expression studies. (A) Flowchart of the DiOGenes dietary intervention. (B) Flowchart of the DiOGenes gene expression analyses (path 1: discovery analyses with the use of RNAseq; path 2: validation analyses with the use of RT-qPCR). CID, clinical investigation day; DiOGenes, Diet, Obesity and Genes; LCD, low-calorie diet; QC, quality control; RT-qPCR, reverse transcription quantitative polymerase chain reaction; RNAseq, RNA sequencing.

Figure 2: Workflow of the samples, data and network analysis. CID, clinical investigation day; DEG, differentially expressed genes; FC, fold change; GMM, Graphical Gaussian Model.

Figure 3: Global network for changes in gene expression and bioclinical parameters during low calorie diet. A sparse Graphical Gaussian Model was used to estimate partial correlations in each set of variables (changes in adipose tissue mRNA level, and changes in bio-clinical parameters during LCD) and mixed models were used to assess links between gene expressions and bio-clinical variables. Network was laid out using force-based algorithms in Gephi 0.9.2 software. The bio-clinical variables are displayed with high size labels. Edge color indicates the correlation sign: red for positive correlations and blue for the negative ones. BMI, body mass index; HDL-Chol, high density lipoprotein; LDL-Chol, low density lipoprotein cholesterol; HOMA-IR, homeostatic model assessment of insulin resistance.

Figure 4: Adipose tissue gene expression using RT-qPCR at all time-points of the dietary intervention. The mRNA levels of *CCL3*, *CD68*, *LIPA*, *GDF15* and *SPP1* were measured in abdominal subcutaneous adipose tissue (n=219-351) at baseline (CID1), after an 8-week low calorie diet (CID2), and after 6

months of weight maintenance diet (CID3). CID, clinical investigation day. ***, $p < 0.001$ from Friedman and Dunn's multiple comparison tests.

Figure 5: Adipose tissue gene expression in human adipose tissue cells. The mRNA level of *CCL3*, *CD68*, *LIPA*, *GDF15* and *SPP1* were measured in abdominal subcutaneous adipose tissue freshly isolated adipocytes (Adipo), preadipocytes (Preadipo), lymphocytes (Lympho) and macrophages (Macro)(n=5). *, $p < 0.05$; **, $p < 0.01$; ***, $p < 0.001$ from Kruskal-Wallis and Dunn's multiple comparison vs. adipocytes tests.

Figure 6: Adipose tissue gene expression in pro- and anti-inflammatory macrophages. The THP-1 cell were induced to M0 macrophages, then polarized to M1-like (pro-inflammatory) or M2-like (anti-inflammatory) phenotype. The mRNA levels of *CCL3*, *CD68*, *LIPA*, *GDF15* and *SPP1* were measured in M0, M1 and M2 macrophages. The data are presented normalized to M0 phenotype (n=11). *, $p < 0.05$; **, $p < 0.01$; ***, $p < 0.001$; ****, $p < 0.0001$ from Mann-Whitney test.

Tables

Table 1 Cohort characteristics

	All (n=416)	Women (n=291)	Men (n=125)	P-value	FDR
Age, y	41.01 +/- 6.35	40.36 +/- 6.39	42.52 +/- 6.01	0.0012	0.0018
Baseline weight, kg	99.69 +/- 17.14	95.59 +/- 15.75	109.37 +/- 16.44	1.42E-13	7.78E-13
Baseline BMI, kg/m ²	34.76 +/- 4.87	34.83 +/- 4.98	34.59 +/- 4.63	0.6298	0.6298
Baseline HOMA-IR	2.93 +/- 2.20	2.73 +/- 2.25	3.38 +/- 2.04	0.0056	0.0069
Baseline total cholesterol, mmol/L	5.02 +/- 0.93	4.93 +/- 0.89	5.23 +/- 0.98	0.0043	0.0059
Baseline LDL, mmol/L	3.14 +/- 0.83	3.03 +/- 0.78	3.38 +/- 0.87	2.19E-04	4.81E-04
Baseline HDL, mmol/L	1.28 +/- 0.31	1.33 +/- 0.32	1.15 +/- 0.27	4.00E-08	1.47E-07
Baseline waist circumference, cm	106.89 +/- 12.75	103.90 +/- 12.19	114.10 +/- 11.13	1.45E-14	1.59E-13
Percentage of weight loss during LCD	-11.06 +/- 2.74	-10.68 +/- 2.41	-11.90 +/- 3.22	0.0004	0.0008
Percentage of weight loss at study termination	-10.79 +/- 5.97	-10.50 +/- 5.83	-11.59 +/- 6.32	0.2160	0.2376

Number corresponds to mean value +/- standard error. The t-test compares differences between men and women. BMI: Body Mass Index, FDR: False Discovery Rate, HOMA-IR: Homeostasis model assessment of insulin resistance, LCD: Low caloric diet.

Figures

Figure 1

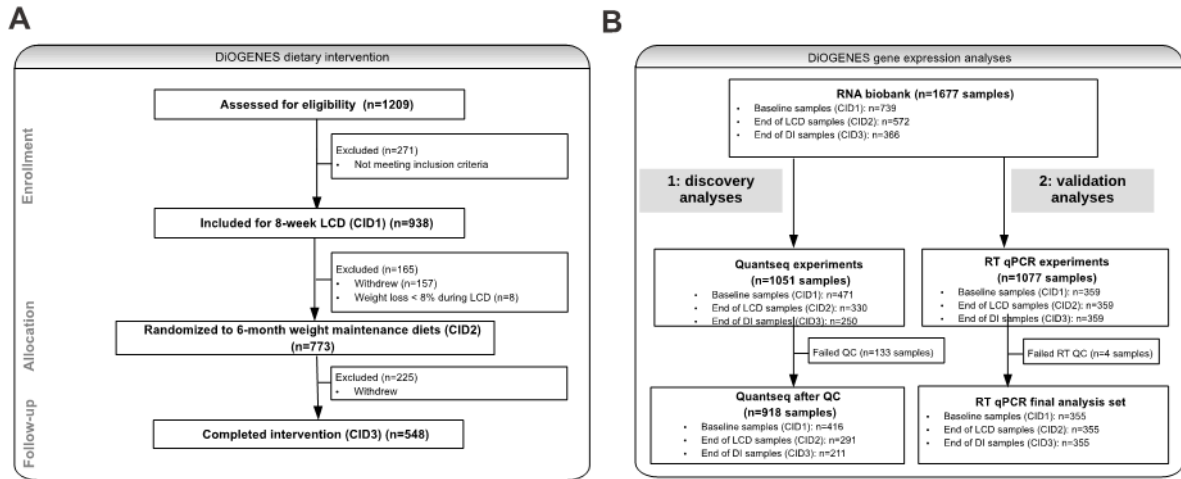


Figure 2

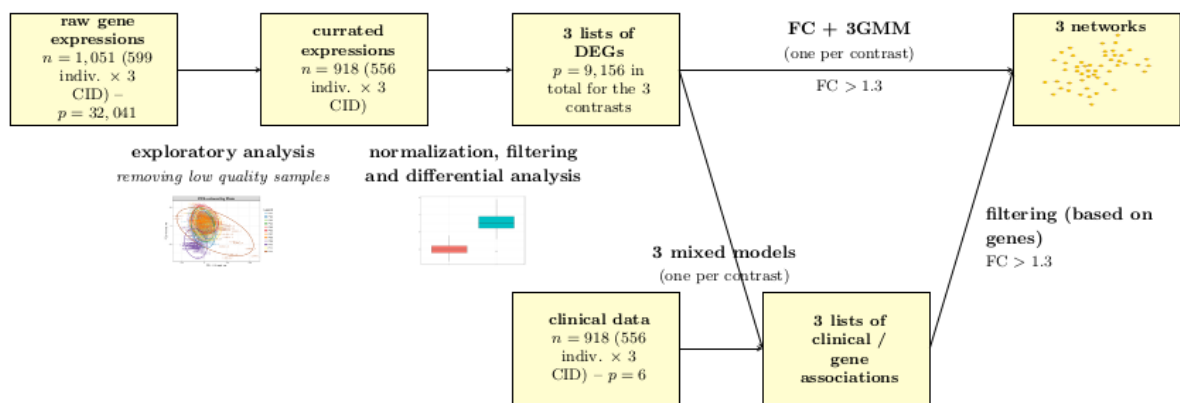


Figure 3

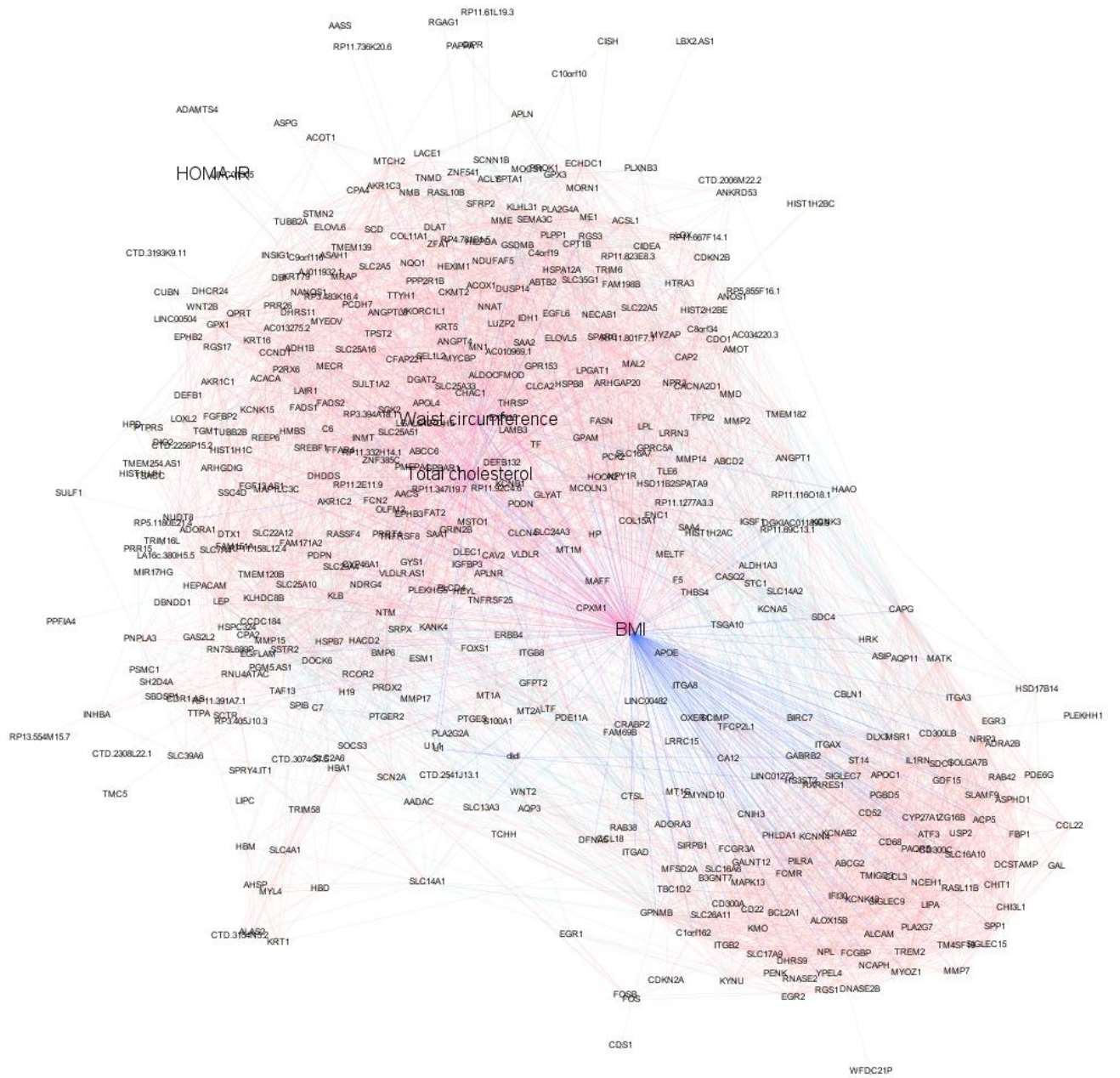


Figure 4

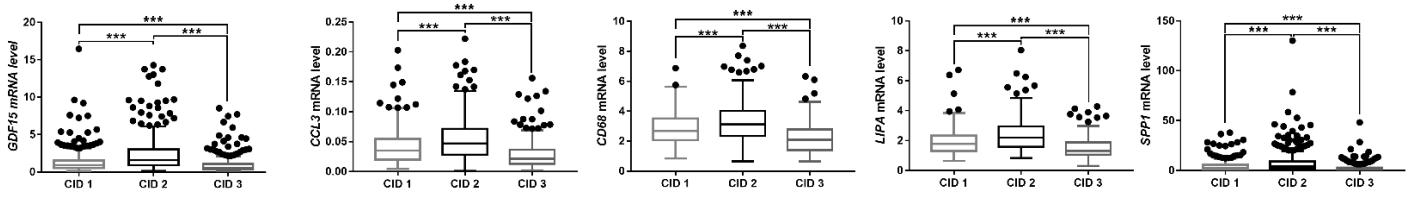


Figure 5

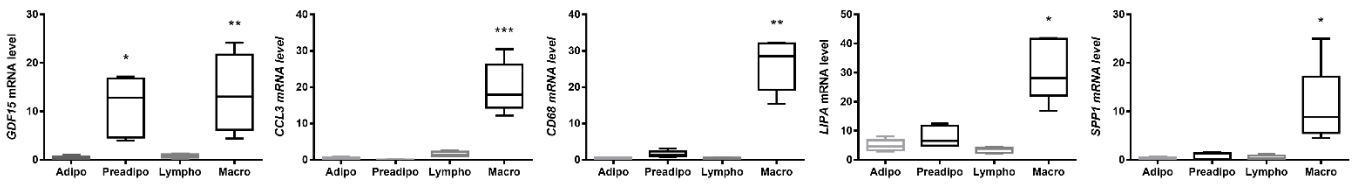


Figure 6

